Inorg. Chem. **2002**, *41*, 5403–5409

Spontaneous Reduction of a Low-Spin Fe(III) Complex of a Neutral Pentadentate N_5 Schiff Base Ligand to the Corresponding Fe(II) Species in Acetonitrile

Apurba K. Patra,[†] Marilyn M. Olmstead,[‡] and Pradip K. Mascharak*,[†]

Department of Chemistry and Biochemistry, University of California, Santa Cruz, California 95064, and the Department of Chemistry, University of California, Davis, California 95616

Received May 29, 2002

The iron complexes of a designed pentadentate Schiff base ligand *N*,*N*-bis(2-pyridylmethyl)amine-*N*-ethyl-2-pyridine-2-aldimine ($SBPy_3$) have been synthesized. The low-spin mononuclear Fe(III) complex $[(SBPy_3)Fe(DMF)](ClO_4)_3$ (**2**), though stable in the solid state, is spontaneously reduced to the corresponding Fe(II) species $[(SBPy_3)Fe(MeCN)]^{2+}$ in MeCN. Fe(II) complex $[(SBPy_3)Fe(MeCN)](BF_4)_2$ (**3**) has been isolated independently and characterized by crystallography. Electrochemical studies indicate that $SBPy_3$, like other pentadentate polypyridine ligands, stabilizes the Fe(II) center to a great extent ($E_{1/2} = 1.01$ V vs SCE in MeCN). This fact is responsible for the ready reduction of **2**. It is evident that such reactivity has brought complications in the syntheses of iron complexes of polypyridine ligands reported in previous accounts. Very low solubility of **2** in MeOH has allowed isolation of analytically pure **2** in the present work. Storage of dilute methanolic solution of **2** results in the formation of the μ-oxo Fe(III) dimer $[(SBPy_3)FeOFe(SBPy_3)](ClO_4)_4$ (**5**), the structure of which has also been determined. Fe(II) complex **3** reacts with CN^- to afford cyanide adduct $[(SBPy_3)Fe(CN)](BF_4)$ (**4**) but does not exhibit any reactivity toward NO. The azomethine moiety (CH═N—py) of **2** is rapidly oxidized by H_2O_2 to a pyridine-2-carboxamido (C(═O)—N—py) unit and affords $[(PaPy_3)Fe(MeCN)](ClO_4)_2$ (**1**), a complex previously reported by us.

Introduction

Scrutiny of the vast coordination chemistry of iron[1−4] reveals that certain ligands provide significant stabilization to the +3 oxidation state while other ligands prefer to bind iron in the +2 state. It is now established that ligands with carboxamide,[5,6] oxime, and carboxylate[7] groups exhibit preference toward Fe(III) centers. Ligands with pyridine and imidazole nitrogens and thioether on the other hand afford stable Fe(II) complexes.[1−4] Therefore, a varying number of these donor groups can be assembled in a designed complex to tune the redox and hydrolytic properties of the iron center.

During the past few years, pentadentate ligands (Figure 1) with neutral N donor centers have drawn attention of the bioinorganic chemists in their pursuit of synthesizing hexacoordinated iron complexes with a labile ligand, usually a solvent molecule, at the sixth site.[6a,8] Studies on the hydroperoxo and/or alkylperoxo adducts of the mononuclear iron

* To whom correspondence should be addressed. E-mail: mascharak@chemistry.ucsc.edu.

[†] Department of Chemistry and Biochemistry, University of California, Santa Cruz.

[‡] Department of Chemistry, University of California, Davis.

(1) (a) Nordlander, E.; Whalen, A. M. *Coord. Chem. Rev.* **1995**, *142*, 43. (b) Nordlander, E.; Whalen, A. M.; Prestopino, F. *Coord. Chem. Rev.* **1995**, *146*, 225. (c) Powel, A. K. *Coord. Chem. Rev.* **1994**, *134*, 91. (d) Thronton, P. *Coord. Chem. Rev.* **1992**, *113*, 131. (e) Cotton, S. A. *Coord. Chem. Rev.* **1972**, *8*, 185.

(2) Nelson, S. M. In *Comprehensive Coordination Chemistry*; Wilkinson, G., Ed.; Pergamon: Oxford, 1987; Vol. 4, pp 217−276. (b) Hawker, P. N.; Twigg, M. V. In *Comprehensive Coordination Chemistry*; Wilkinson, G., Ed.; Pergamon: Oxford, 1987; Vol. 4, pp 1179−1288.

(3) Nicholls, D. In *Comprehensive Inorganic Chemistry*; Bailar, J. C., Jr., Emeleus, H. J., Nyholm, R., Trotman-Dickenson, A. F., Eds.; Pergamon: Oxford, 1973; Vol. 3, pp 979−1051.

(4) *Encyclopedia of Inorganic Chemistry*; King, R. B., Ed.; Wiley: New York; Vol 4.

(5) Marlin, D. S.; Mascharak, P. K. *Chem. Soc. Rev.* **2000**, *29*, 69.

(6) (a) Rowland, J. M.; Olmstead, M.; Mascharak, P. K. *Inorg. Chem.* **2001**, *40*, 2810. (b) Noveron, J. C.; Olmstead M. M.; Mascharak, P. K. *J. Am. Chem. Soc.* **2001**, *123*, 3247. (c) Marlin, D. S.; Olmstead, M. M.; Mascharak, P. K. *Inorg. Chem.* **1999**, *38*, 3258. (d) Noveron, J. C.; Olmstead M. M.; Mascharak, P. K. *Inorg. Chem.* **1998**, *37*, 1138. (e) Nguyen, C.; Guajardo, R. J.; Mascharak, P. K. *Inorg. Chem.* **1996**, *21*, 6273.

(7) (a) Mizoguchi, T. J.; Kuzelka, J.; Spingler, B.; Dubois, J.; Davydov, R. M.; Hedman, B.; Hodgson, K. O.; Lippard, S. J. *Inorg. Chem.* **2001**, *40*, 4662. (b) Dubois, J.; Mizoguchi, T. J.; Lippard, S. J. *Coord. Chem. Rev.* **2000**, *200*−*202*, 443.

10.1021/ic020373w CCC: $22.00
Published on Web 09/06/2002

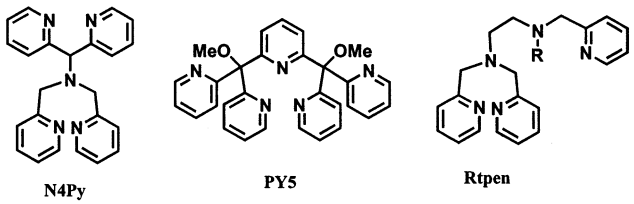

Figure 1. Pentadentate N_5 ligands (L) used to synthesize $[LFe(solv)]^{n+}$ species.

complexes of these pentadentate ligands have provided valuable insight related to the spectroscopic properties and reactivities of non-heme iron-containing oxygenases.[8d] Mononuclear iron complexes, derived from tris-(2-pyridylmethyl)-amine (TPA), have also been used in similar studies.[9] It is important to note that these polypyridine ligands afford primarily Fe(II) complexes of the type $[(L)Fe(solv)]^{2+}$ (L = ligand) where the solvent (solv) is either acetonitrile (MeCN) or methanol (MeOH).[10]

Recently, we have reported a designed pentadentate ligand, namely *N*,*N*-bis(2-pyridylmethyl)amine-*N*-ethyl-2-pyridine-2-carboxamide ($PaPy_3H$, H is the dissociable amide proton), which comprises a carboxamide group in its frame.[6a] Quite in contrast to the ligands shown in Figure 1, $PaPy_3H$ readily affords the Fe(III) complex $[(PaPy_3)Fe(MeCN)](ClO_4)_2$ (**1**). This change in oxidation state preference arises from coordination of the carboxamido nitrogen which, as shown previously by us,[5,6] provides significant stability to Fe(III) center. Indeed, the half-wave potential ($E_{1/2}$) of the Fe(II)/Fe(III) couple of **1** in MeCN is 0.21 V (vs saturated calomel electrode, SCE) while $[(N4Py)Fe(MeCN)](ClO_4)_2$ and $[(Py5)Fe(MeCN)](ClO_4)_2$ exhibit $E_{1/2}$ values of 1.01 and 1.21 V (vs SCE), respectively, in the same solvent.[8c,e] The shift of over 0.8 V in the $E_{1/2}$ value due to ligation by one carboxamido nitrogen is quite striking.

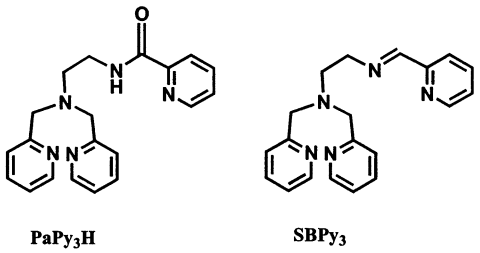

To further establish this effect of the coordinated carboxamido nitrogen in **1**, we have now synthesized Schiff base ligand *N*,*N*-bis(2-pyridylmethyl)amine-*N*-ethyl-2-pyridine-2-aldimine ($SBPy_3$) which is identical to $PaPy_3H$ except for the fact that it has an imine group in place of the carboxamide moiety. In this paper, we report the syntheses of $SBPy_3$ and its iron complexes. The results confirm that $SBPy_3$ stabilizes Fe(II) (and not Fe(III)) to a great extent much like the ligands of Figure 1 because there is no carboxamide group in the ligand frame. Although we have been able to isolate the Fe(III) complex, $[(SBPy_3)Fe(DMF)](ClO_4)_3$ (**2**, DMF = dimethylformamide), it is difficult to keep this species in solution, and in solvents such as MeCN and DMF, *it is spontaneously reduced to the corresponding Fe(II) complex*, $[(SBPy_3)Fe(solv)]^{2+}$. Fe(II) complex $[(SBPy_3)Fe(MeCN)](BF_4)_2$ (**3**), prepared independently, exhibits an $E_{1/2}$ value (1.01 V vs SCE in MeCN) identical to that of $[(N4Py)Fe(MeCN)](ClO_4)_2$. Other complexes of $SBPy_3$ are also discussed.

Experimental Section

2-Aminomethylpyridine, N-bromoethylphthalimide, picolinic acid, hydrazine monohydrate, 2-pyridinecarboxaldehyde, and hydrogen peroxide (30%) were purchased from Aldrich Chemical Co. and used without further purification. The Fe(III) starting material, $[Fe(DMF)_6](ClO_4)_3$, and (2-aminoethyl)bis(2-pyridylmethyl)amine (DPEA) were synthesized by following published procedures.[11,12] MeCN, DMF, MeOH, and diethyl ether (Et_2O) were obtained from Fischer Chemical Co. and were distilled from CaH_2, BaO, $Mg(OEt)_2$, and sodium/benzophenone, respectively, prior to use.

Synthesis Safety Note. Transition metal perchlorates should be handled with great caution and be prepared in small quantities as metal perchlorates are hazardous and may explode upon heating.

Synthesis of Compounds. *N*,*N*-Bis(2-pyridylmethyl)amine-*N*-ethyl-2-pyridine-2-aldimine ($SBPy_3$). A solution of 0.48 g (4.48 mmol) of 2-pyridinecarboxaldehyde in 10 mL of MeOH was added slowly to a solution of 1.08 g (4.46 mmol) of DPEA in 10 mL of MeOH, and the reaction mixture was heated to reflux under dinitrogen for 5 h. Next, the solvent was removed completely under vacuum, and the brown oil was redissolved in 20 mL of chloroform ($CHCl_3$). The solution was then washed several times with distilled water, and the $CHCl_3$ layer was dried with anhydrous Na_2SO_4. Removal of $CHCl_3$ afforded pure $SBPy_3$ as a light yellow oil (1.40 g, 95%). ^1H NMR (303 K, $CDCl_3$, 500 MHz): δ (ppm from TMS), 8.64 (d 1H), 8.52 (d 2H), 8.34 (s 1H), 7.94 (d 1H), 7.74 (t 1H), 7.58 (t 2H), 7.52 (d 2H), 7.32 (t 1H), 7.12 (t 2H), 3.94 (s 4H), 3.85 (t 2H), 2.98 (t 2H). Selected IR frequency (NaCl plate): $\nu_{C=N}$ 1649 cm^{-1}.

$[(SBPy_3)Fe(DMF)](ClO_4)_3$ (2). Under dinitrogen, a slurry of 0.50 g (0.63 mmol) of $[Fe(DMF)_6](ClO_4)_3$ in 20 mL of MeOH was slowly added to a solution of 0.21 g (0.63 mmol) of $SBPy_3$ in 10 mL of MeOH, and the mixture was stirred. The reaction mixture rapidly became homogeneous, and complex **2** separated out from the red solution as a red microcrystalline solid within minutes. The solid was filtered, washed with anhydrous Et_2O, and dried in a vacuum (0.26 g, 57% yield). Anal. Calcd for $C_{24}H_{32}Cl_3FeN_6O_{14}$ (**2**·MeOH): C, 36.45; H, 4.08; N, 10.63. Found: C, 36.31; H, 4.11; N, 10.73. Selected IR frequencies (in cm^{-1}, KBr disk): 3425 (br, m), 3072 (w), 2932 (w), 2791 (w), 1650 (m), 1602 (m), 1479 (w), 1437 (m), 1291 (m), 1090 (ClO_4, vs), 774 (s), 620 (s). Electronic

(8) (a) Hazell, A.; McKenzie, C. J.; Nielson, L. P.; Schindler, S.; Weitzer, M. *J. Chem. Soc., Dalton. Trans.* **2002**, 310. (b) Wada, A.; Ogo, S.; Nagatomo, S.; Kitagawa, T.; Watanabe, Y.; Jitsukawa, K.; Masuda, H. *Inorg. Chem.* **2002**, *41*, 616. (c) Goldsmith, C. R.; Jonas, R. T.; Stack, T. D. P. *J. Am. Chem. Soc.* **2002**, *124*, 83. (d) Girerd, J.-J.; Banse, F.; Simaan, A. J. *Struct. Bonding (Berlin)* **2000**, *97*, 145. (e) Roelfes, G.; Lubben, M.; Chen, K.; Ho, R. Y. N.; Meetsma, A.; Genseberger, S.; Hermant, R. M.; Hage, R.; Mandal, S. K.; Young, V. G., Jr.; Zang, Y.; Kooijmannn, H.; Spek, A. L.; Que, L., Jr.; Feringa, B. L. *Inorg. Chem.* **1999**, *38*, 1929.

(9) (a) Chen, K.; Costas, M.; Kim, J.; Tipton, A. K.; Que, L., Jr. *J. Am. Chem. Soc.* **2002**, *124*, 3026. (b) Costas, M.; Tipton, A. K.; Chen, K.; Jo, D.-H.; Que, L., Jr. *J. Am. Chem. Soc.* **2001**, *123*, 6722.

(10) Fe(III) complexes of the type $[(L)Fe(X)]^{2+}$ (where X = anion like OMe^-) with these ligands have been reported. For example, see refs 8c,e.

(11) Hodgkinson, J.; Jordan, R. B. *J. Am. Chem. Soc.* **1973**, *95*, 763.

(12) Matouzenko, G. S.; Bousseksou, A.; Lecocq, S.; van Koningsbruggen, P. J.; Perrin, M.; Kahn, O.; Collet, A. *Inorg. Chem.* **1997**, *36*, 2975.

absorption spectrum in MeCN (freshly prepared) λ_{max} (in nm) (ϵ in M^{-1} cm^{-1}): 545 sh (1 500), 445 sh (2470), 390 sh (4240), 345 (5420). Value of μ_{eff} (298 K, polycryst): 2.01 μ_B. X-band EPR spectrum in 1:1 methanol/acetone glass (86 K): $g = 2.313$, 2.157, and 1.933.

[(SBPy$_3$)Fe(MeCN)](BF$_4$)$_2$·1/3Et$_2$O·2/3MeOH (3·1/3Et$_2$O·2/3MeOH). Under dinitrogen, a solution of 0.20 g (0.59 mmol) of [Fe(H$_2$O)$_6$](BF$_4$)$_2$ in 10 mL of MeOH was added to a solution of 0.20 g (0.60 mmol) of SBPy$_3$ in 7 mL of MeOH, and the deep purple solution was stirred for 1 h. Next, 3 mL of MeCN was added to it, and anhydrous Et$_2$O was allowed to diffuse into this mixture at 4 °C. Magenta plates of [(SBPy$_3$)Fe(MeCN)](BF$_4$)$_2$·1/3Et$_2$O·2/3MeOH (**2**·1/3 Et$_2$O·2/3MeOH) were isolated after 4 days (0.27 g, 70% yield). Anal. Calcd for $C_{24}H_{30}B_2F_8FeN_6O$ (**2**·1/3Et$_2$O·2/3MeOH): C, 44.48; H, 4.67; N, 12.97. Found: C, 44.21; H, 4.81; N, 12.73. Selected IR frequencies (in cm^{-1}, KBr disk): 3427 (br, m), 1605 (m), 1460 (m), 1294 (w), 1054 (BF$_4$, vs), 771 (m), 523 (m). Electronic absorption spectrum λ_{max} (in nm) (ϵ in M^{-1} cm^{-1}): in MeOH, 570 (4030), 395 (5690), 280 (8730), 257 (11 870); in MeCN, 557 (6780), 385 (10 560), 280 (10 820), 252 (16 830). ^{1}H NMR (500 MHz, CD$_3$CN, δ from TMS): 9.28 (s, 1H), 8.97 (d, 1H), 8.31 (d, 2H), 8.24 (t, 3H), 7.80 (m, 2H), 7.42 (d, 2H), 7.09 (t, 2H), 6.56 (d, 2H), 4.92 (d, 2H), 4.71 (d, 2H), 3.82 (t, 2H), 3.18 (t, 2H).

[(SBPy$_3$)Fe(CN)](BF$_4$)·MeCN (4·MeCN). A solution of 0.029 g (0.18 mmol) of NEt$_4$CN in 2 mL of MeCN was added dropwise to a deep purple solution of 0.10 g (0.17 mmol) of complex **3** in 5 mL of MeCN. The color changed from deep purple to deep green when addition of the NEt$_4$CN was complete. The deep green solution was stirred for 1 h. Diffusion of Et$_2$O to this green solution at 4 °C afforded deep green crystals (0.075 g, 83%) within 48 h. Anal. Calcd for $C_{23}H_{24}BF_4FeN_7$ (**4**·MeCN): C, 51.05; H, 4.47; N, 18.12. Found: C, 50.98; H, 4.43; N, 18.01. Selected IR frequencies (in cm^{-1}, KBr disk): 2073 (CN$^-$, s), 1596 (m), 1460 (s), 1432(s), 1294(w), 1055 (BF$_4$, vs), 781 (m), 514 (w). Electronic absorption spectrum λ_{max} (in nm) (ϵ in M^{-1} cm^{-1}): in MeCN, 595 (8554), 410 (11 733), 280 (11 386), 252 (14 334). ^{1}H NMR (500 MHz, CD$_3$CN, δ from TMS): 9.55 (s, 1H), 9.26 (d, 1H), 8.21 (d, 1H), 8.04 (t, 1H), 7.65 (m, 3H), 7.28 (d, 2H), 6.95 (t, 2H), 6.31 (d, 2H), 4.67 (dd, 4H), 4.02 (t, 2H), 3.04 (t, 2H).

[(SBPy$_3$)FeOFe(SBPy$_3$)](ClO$_4$)$_4$·1.2(Me)$_2$CO·0.8H$_2$O (5·1.2(Me)$_2$CO·0.8H$_2$O). A solution of 0.03 g of 40% NEt$_4$OH (40 wt % solution in water, 0.079 mmol) in 8 mL of 1:1 (v/v) MeCN/MeOH was slowly added to a slurry of 0.06 g (0.079 mmol) of [(SBPy$_3$)Fe(DMF)](ClO$_4$)$_3$ in 10 mL of MeOH with constant stirring. The reaction mixture became homogeneous within minutes, and the red solution thus obtained was stirred for 5 h. Slow evaporation of the solvent from this reaction mixture afforded a batch of microcrystalline red-brown solid. The crystals were collected by filtration, washed with dry acetone ((Me)$_2$CO), and finally dried in air (0.030 g, 64%). Crystals suitable for X-ray diffraction were grown from a DMF/(Me)$_2$CO mixture. Anal. Calcd for $C_{43.6}H_{50.8}Cl_4Fe_2N_{10}O_{19}$ (**4**·1.2 (Me)$_2$CO·0.8H$_2$O): C, 41.15; H, 4.02; N, 11.01. Found: C, 40.78; H, 3.97; N, 11.16. Selected IR frequencies (in cm^{-1}, KBr disk): 3412 (br, m), 1648 (w), 1607 (m), 1478 (w), 1090 (ClO$_4$, vs), 808 (m), 784 (m), 620(m). Electronic absorption spectrum λ_{max} (in nm) (ϵ in M^{-1} cm^{-1}): in MeCN, 366 (sh 7220), 310 (sh 11 830), 252 (38 130).

Physical Measurements. Absorption spectra were recorded on a Varian Cary 50 spectrophotometer. A Perkin-Elmer 1600 FTIR spectrophotometer was employed to monitor the infrared spectra. X-band EPR spectra were obtained with a Bruker ESP-300 spectrometer. Electrochemical studies were performed with Princeton Applied Research instrumentation in MeCN using 0.1 M tetraethylammonium perchlorate as the supporting electrolyte. The working electrode was a Beckman Pt-inlay working electrode, and the potentials were measured versus a saturated calomel electrode (SCE). ^{1}H NMR spectra were recorded at 298 K on a Varian 500 MHz spectrometer.

Table 1. Summary of Crystal Data and Intensity Collection and Structural Refinement Parameters for [(SBPy$_3$)Fe(MeCN)](BF$_4$)$_2$·1/3Et$_2$O·2/3MeOH (**3**·1/3Et$_2$O·2/3MeOH), [(SBPy$_3$)Fe(CN)](BF$_4$)·MeCN (**4**·MeCN), and [(SBPy$_3$)FeOFe(SBPy$_3$)](ClO$_4$)$_4$·1.2(Me)$_2$CO·0.8H$_2$O (**5**·1.2(Me)$_2$CO·0.8H$_2$O)

	3	**4**	**5**
formula	$C_{24}H_{30}B_2F_8FeN_6O$	$C_{23}H_{24}BF_4FeN_7O$	$C_{43.6}H_{50.8}Cl_4Fe_2N_{10}O_{19}$
mol wt	648.01	541.15	1272.44
cryst color, habit	magenta plate	green needle	red-brown plate
T, K	91(2)	91(2)	91(2)
cryst syst	monoclinic	triclinic	triclinic
space group	*C*2/*c*	$P\bar{1}$	$P\bar{1}$
a, Å	38.398(15)	8.9246(17)	12.543(5)
b, Å	11.859(5)	12.091(2)	13.258(6)
c, Å	12.783(5)	12.244(2)	19.381(8)
α, deg	90	109.275(4)	94.408(15)
β, deg	103.422(8)	92.743(4)	95.638(17)
γ, deg	90	97.343(7)	115.82(2)
V, Å^3	5662(4)	1231.2(4)	2861(2)
Z	8	2	2
d_{calcd}, g cm^{-3}	1.520	1.460	1.477
abs coeff, μ, mm^{-1}	0.616	0.669	0.772
GOF[a] on F^2	1.026	1.042	1.029
R1,[b] %	6.07	4.01	8.96
wR2,[c] %	15.32	10.66	24.07

[a] GOF = $[\sum w(F_o^2 - F_c^2)^2]/(M - N)]^{1/2}$ (M = number of reflections, N = number of parameters refined). [b] R1 = $\sum||F_o| - |F_c||/\sum|F_o|$. [c] wR2 = $[\sum[w(F_o^2 - F_c^2)^2]/\sum[w(F_o)^2]]^{1/2}$.

X-ray Data Collection and Structure Solution and Refinement. Magenta plates of complex **3**·1/3Et$_2$O·2/3MeOH were obtained from a solution of the complex in MeOH/MeCN (7:3, v/v) via diffusion of Et$_2$O at 4 °C. Deep green needles of **4**·MeCN were grown from a MeCN solution of the complex while diffusion of (Me)$_2$CO into a solution of **5** in DMF/MeOH (1:10 v/v) afforded red-brown crystals of **5**·1.2(Me)$_2$COMe·0.8H$_2$O. Diffraction data for the complexes were collected at 91 K on a Bruker SMART 1000 system. Mo Kα (0.710 73 Å) radiation was used, and the data were corrected for absorption. The structures were solved by direct methods (standard SHELXS-97 package). Machine parameters, crystal data, and data collection parameters for all the complexes are summarized in Table 1 while selected bond distances and angles are listed in Tables 2 and 3. Complete crystallographic data for [(SBPy$_3$)Fe(MeCN)](BF$_4$)$_2$·1/3Et$_2$O·2/3MeOH (**3**·1/3Et$_2$O·2/3MeOH), [(SBPy$_3$)Fe(CN)](BF$_4$)·MeCN (**4**·MeCN), and [(SBPy$_3$)FeOFe(SBPy$_3$)](ClO$_4$)$_4$·1.2(Me)$_2$CO·0.8H$_2$O (**5**·1.2(Me)$_2$CO·0.8H$_2$O) have been submitted as Supporting Information.

Results and Discussion

Synthesis. The Schiff base ligand SBPy$_3$ serves as a pentadentate ligand in all four complexes (**2**−**5**) reported in this account, and much like the ligands of Figure 1, it employs three pyridine nitrogens, one *tert*-amine nitrogen, and one imine nitrogen to bind iron in these complexes. Among the iron complexes of SBPy$_3$, mononuclear Fe(III) species **2** is quite unstable in solution. Isolation of this

Table 2. Selected Bond Distances [Å] and Bond Angles [deg] for $[(SBPy_3)Fe(MeCN)](BF_4)_2 \cdot 1/3Et_2O \cdot 2/3MeOH$ (**3**·1/3Et$_2$O·2/3MeOH) and $[(SBPy_3)Fe(CN)](BF_4) \cdot MeCN$ (**4**·MeCN)

complex **3**		complex **4**	
Fe−N1	1.974(3)	Fe−N1	1.9588(13)
Fe−N2	1.878(2)	Fe−N2	1.9022(13)
Fe−N3	1.996(3)	Fe−N3	1.9922(13)
Fe−N4	1.965(2)	Fe−N4	1.9664(13)
Fe−N5	1.973(3)	Fe−N5	1.9769(13)
Fe−N6	1.960(2)	Fe−C21	1.9465(16)
N2−C6	1.284(4)	N2−C6	1.2846(19)
N6−C21	1.136(4)	C21−N6	1.161(2)
C21−C22	1.467(4)	N3−C8	1.5083(19)
N1−Fe−N2	81.19(11)	N1−Fe−N2	81.00(5)
N1−Fe−N3	166.71(10)	N1−Fe−N3	165.97(5)
N1−Fe−N4	97.83(10)	N1−Fe−N4	98.41(6)
N1−Fe−N5	96.44(10)	N1−Fe−N5	95.85(5)
N1−Fe−N6	96.54(10)	N1−Fe−C21	96.02(6)
N2−Fe−N3	85.88(11)	N2−Fe−N3	85.43(5)
N2−Fe−N4	88.23(10)	N2−Fe−N4	86.47(5)
N2−Fe−N5	94.41(11)	N2−Fe−N5	94.80(5)
N2−Fe−N6	177.02(11)	N2−Fe−C21	174.67(6)
N3−Fe−N4	84.76(10)	N3−Fe−N4	84.25(5)
N3−Fe−N5	81.44(11)	N3−Fe−N5	81.67(5)
N3−Fe−N6	96.48(10)	N3−Fe−C21	97.78(6)
N4−Fe−N5	165.72(10)	N4−Fe−N5	165.71(6)
N4−Fe−N6	90.17(10)	N4−Fe−C21	89.62(6)
N5−Fe−N6	87.76(10)	N5−Fe−C21	89.88(6)
Fe−N6−C21	177.1(3)	Fe−C21−N6	175.97(14)
N6−C21−C22	179.4(4)	N3−C8−C7	110.42(12)

Table 3. Selected Bond Distances [Å] and Bond Angles [deg] for $[(SBPy_3)FeOFe(SBPy_3)](ClO_4)_4 \cdot 1.2(Me)_2CO \cdot 0.8H_2O$ (**5**·1.2(Me)$_2$CO·0.8H$_2$O)

Fe1−N1	2.133(5)	Fe2−N6	2.139(5)
Fe1−N2	2.139(5)	Fe2−N7	2.145(5)
Fe1−N3	2.222(5)	Fe2−N8	2.217(5)
Fe1−N4	2.143(5)	Fe2−N9	2.128(5)
Fe1−N5	2.137(5)	Fe2−N10	2.145(5)
Fe1−O1	1.796(4)	Fe2−O1	1.809(4)
N2−C6	1.270(7)	N7−C26	1.272(8)
N1−Fe−N2	74.74(19)	N6−Fe2−N7	74.57(18)
N1−Fe1−N3	151.10(19)	N6−Fe2−N8	150.58(18)
N1−Fe1−N4	98.4(2)	N6−Fe2−N9	106.27(18)
N1−Fe1−N5	104.65(19)	N6−Fe2−N10	97.05(19)
N1−Fe1−O1	100.43(19)	N6−Fe2−O1	100.20(18)
N2−Fe1−N3	77.12(18)	N7−Fe2−N8	77.22(18)
N2−Fe1−N4	90.66(18)	N7−Fe2−N9	80.94(18)
N2−Fe1−N5	81.38(18)	N7−Fe2−N10	91.02(18)
N2−Fe1−O1	173.46(18)	N7−Fe2−O1	173.32(18)
N3−Fe1−N4	75.4(2)	N8−Fe2−N9	77.05(19)
N3−Fe1−N5	77.22(19)	N8−Fe2−N10	75.20(2)
N3−Fe1−O1	108.12(18)	N8−Fe2−O1	108.51(18)
N4−Fe1−N5	152.5(2)	N9−Fe2−N10	152.1(2)
N4−Fe1−O1	94.45(19)	N9−Fe2−O1	96.81(18)
N5−Fe1−O1	95.81(18)	N10−Fe2−O1	93.79(18)
Fe1−O1−Fe2	175.4(2)	C6−N2−C7	124.1(5)

complex has been possible because mixing of $SBPy_3$ with $[Fe(DMF)_6](ClO_4)_3$ in methanol affords a clear red solution from which **2** precipitates out within minutes. All attempts to synthesize this complex in other solvents (like MeCN or DMF) have failed so far. When the synthesis is performed in MeCN or DMF, the initial red color turns purple, and only **3** is isolated from the reaction mixture. It is quite clear that rapid precipitation of the initial Fe(III) complex **2** from the reaction mixture allows one to isolate **2** from MeOH in an analytically pure form. The stability of **2** in MeOH is quite limited; attempts to crystallize **2** from dilute methanolic solution only afford the μ-oxo dimer, **5**. Spontaneous

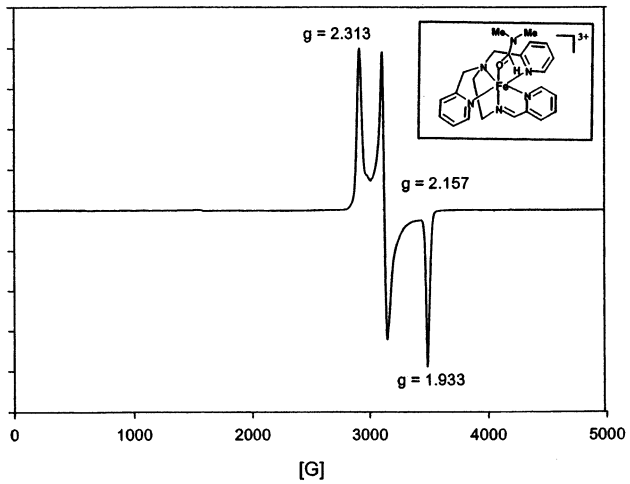

Figure 2. X-band EPR spectrum of **2** in acetone/methanol (1:1) glass (86 K). Spectrometer settings: microwave power, 13 mW; microwave frequency, 9.43 GHz; modulation frequency, 100 kHz; modulation amplitude, 2 G. Inset: structure of $[(SBPy_3)Fe(DMF)]^{3+}$ (cation of **2**).

reduction of **2** to **3** in solvents such as MeCN is a novel reaction that is discussed in detail in a forthcoming section. The instability of **2** in solution did not allow us to determine the structure of **2** in the present work although other spectroscopic properties have allowed us to assign its correct structure. Also, in the solid state, **2** is stable for months and hence is amenable for various other reactions.

That $SBPy_3$ resembles the ligands of Figure 1 is supported by the ease with which one can isolate Fe(II) complex **3**. Reaction of Fe(II) salts and $SBPy_3$ in MeOH or MeCN readily affords $[(SBPy_3)Fe(solv)]^{2+}$ in high yields. The solvent (MeCN) of $[(SBPy_3)Fe(MeCN)](BF_4)_2$ (**3**) can be easily substituted by other ligands. For example, cyanide adduct **4** is obtained upon addition of CN^- to **3**. And finally, prolonged storage of dilute solutions of **2** in MeOH affords μ-oxo dimer **5**. This reaction was discovered while we were trying to isolate crystals of **2** for diffraction studies. As expected, the presence of OH^- in such solutions improves the yield of **5** significantly.

Structure and Properties. $[(SBPy_3)Fe(DMF)](ClO_4)_3$ (2). The instability of this complex in common solvents prevented isolation of crystals suitable for diffraction studies. However, microanalytical data confirmed its composition. In addition, the structure of the corresponding Fe(II) complex, **3**, formed spontaneously upon dissolving **2** in MeCN, supports the structure of Fe(III) precursor **2** which is shown in the inset of Figure 2. A strong IR band at 1650 cm^{-1} indicates the presence of a bound DMF molecule at the sixth site of iron. Ligation of the imine nitrogen to Fe(III) in **2** is confirmed by the red shift of the $\nu_{C=N}$ frequency from 1649 cm^{-1} in free $SBPy_3$ to 1607 cm^{-1} in the complex. The low-spin nature of the Fe(III) center in **2** is supported by its magnetic susceptibility value at room temperature as well as the strong rhombic EPR signal with $g = 2.313$, 2.157, and 1.933 at 86 K (Figure 2).[6a] Fe(III) complexes of Schiff base ligands with N,O donors are either high spin ($S = {}^5/_2$) or exhibit spin equilibria.[13] Complex **2** is unique in this regard and resembles **1** and other Fe(III) complexes of Schiff base ligands with N,S donor atoms.[6a,14]

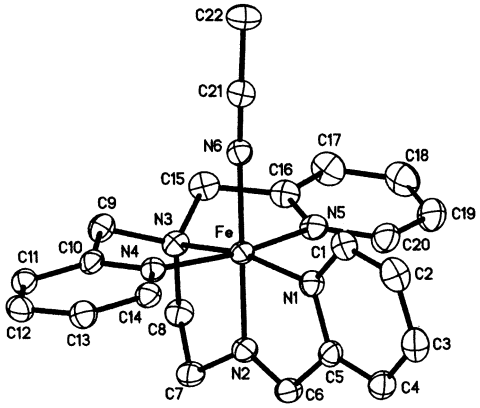

Figure 3. Thermal ellipsoid plot (50% probability level) of $[(SBPy_3)Fe(MeCN)]^{2+}$ (cation of **3**) with the atom numbering scheme. The hydrogen atoms are omitted for the sake of clarity.

$[(SBPy_3)Fe(MeCN)](BF_4)_2\cdot 1/3Et_2O\cdot 2/3MeOH$ ($3\cdot 1/3Et_2O\cdot 2/3MeOH$). The structure of the cation of Fe(II) complex **3** is shown in Figure 3, and selected metric parameters are listed in Table 2. The coordination geometry around Fe(II) is distorted octahedral. The ligand $SBPy_3$ employs three pyridine nitrogens, one imine nitrogen, and one *tert*-amine nitrogen to bind the Fe(II) center while one MeCN molecule occupies the sixth site. It is important to note that the disposition of the pyridine nitrogens and the *tert*-amine nitrogen around iron in **3** is identical to that observed previously in **1**.[6a] Thus, the two ligands $PaPy_3^-$ and $SBPy_3$ coordinate to iron in the same conformation. This mode of ligation places the imine nitrogen trans to the bound MeCN molecule in **3** while in **1** the carboxamido nitrogen is trans to the bound MeCN molecule.

The Fe(II)−N distances in **3** (Table 2) are comparable to the Fe(II)−N distances reported for other similar low-spin Fe(II) complexes such as $[(TPA)Fe(MeCN)_2]^{2+}$,[15] $[(N4Py)Fe(MeCN)]^{2+}$,[8e] and $[(PY5)Fe(MeCN)]^{2+}$.[16] For example, the Fe(II)−$N_{(tert\text{-amine})}$ distance of **3** (1.996 Å) is almost identical to the Fe(II)−$N_{(tert\text{-amine})}$ distance of $[(TPA)Fe(MeCN)_2]^{2+}$ (1.99(1) Å),[15] while the average Fe(II)−N_{py} (py = pyridine) distance (1.970 Å) of **3** is identical to that noted for $[(N4Py)Fe(MeCN)]^{2+}$.[8e] In **3**, the Fe(II)−N_{imine} bond is 1.878(2) Å long. This distance is comparable to other Fe(II)−N_{imine} bond distances in Fe(II) complexes of Schiff base ligands.[17] Finally, the Fe(II)−$N_{(MeCN)}$ bond distance in **3** (1.960(2) Å) is noticeably longer than the same distance in $[(N4Py)Fe(MeCN)]^{2+}$ (1.915(3) Å) and $[(TPA)Fe(MeCN)_2]^{2+}$ (average: 1.925(1) Å). This lengthening of the Fe(II)−$N_{(MeCN)}$ bond in **3** presumably arises from stronger trans influence of the imine nitrogen compared to *tert*-amine nitrogen.

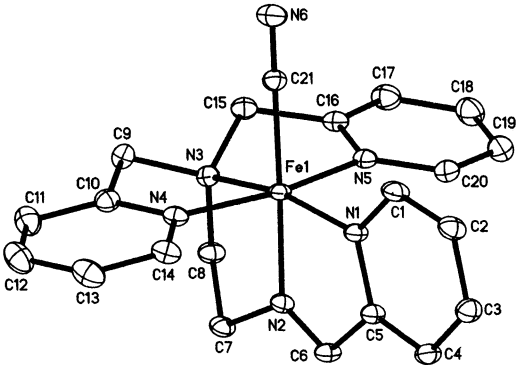

Figure 4. Thermal ellipsoid plot (50% probability level) of $[(SBPy_3)Fe(CN)]^+$ (cation of **4**) with the atom numbering scheme. Hydrogen atoms are omitted for the sake of clarity.

Coordination of the imine nitrogen to Fe(II) in **3** is indicated by the red shift of the $\nu_{C=N}$ frequency from 1649 cm^{-1} in free $SBPy_3$ to 1605 cm^{-1} in the complex. The deep purple color of **3** arises from a strong absorption band in the visible region (λ_{max}: 557 nm in MeCN, 570 nm in MeOH). This band arises from a metal-to-ligand charge transfer (MLCT) because the absorption maximum red shifts to 595 nm in MeCN upon addition of CN^- (vide infra). The low-spin nature of the Fe(II) center in **3** is supported by the clean ^1H NMR spectrum in solvents such as CD_3CN (Figure S1, Supporting Information). Ligation of $SBPy_3$ provides exceptional stability to the Fe(II) center in **3**. For example, in MeCN, **3** exhibits a reversible cyclic voltammogram with $E_{1/2}$ of 1.01 V (vs SCE). This value is in the range of the $E_{1/2}$ values of the Fe(II) complexes of the ligands of Figure 1. For example, the $E_{1/2}$ values of $[(N4Py)Fe(MeCN)]^{2+}$ and $[(PY5)Fe(MeCN)]^{2+}$ are 1.01 and 1.21 V (vs SCE, in MeCN), respectively.

$[(SBPy_3)Fe(CN)](BF_4)\cdot MeCN$ ($4\cdot MeCN$). The structure of $[(SBPy_3)Fe(CN)]^+$, the cation of **4**, is shown in Figure 4, and the selected bond distances and angles are included in Table 2. The coordination geometry around Fe(II) is distorted octahedral, and the coordination mode of the ligand $SBPy_3$ is identical to that in **3**. Substitution of the coordinated MeCN molecule by CN^- introduces very little change in the metric parameters of **4** except for the lengthening of the Fe(II)−N_{imine} distance (1.9022(13) Å) due to the trans influence of CN^-. The Fe(II)−(CN) distance of **4** (1.9465(16) Å) is comparable to the same distance in other low-spin Fe(II) complexes with coordinated cyanide.[18]

A strong ν_{CN} at 2073 cm^{-1} in the IR spectrum indicates the presence of the coordinated CN^- in **4**. The deep green color of **4** in MeCN arises from a strong absorption band with maximum at 595 nm. As mentioned before, this MLCT absorption shifts from 557 nm in the case of **3** to 595 nm in the case of **4**. Coordination of CN^- clearly assists metal-to-ligand charge transfer by providing more electron density to the metal center. Electrochemical data indicate that the

(13) (a) Ramesh, K.; Mukherjee, R. *J. Chem. Soc., Dalton Trans*. **1992**, 83. (b) Costes, J.-P.; Dahan, F.; Laurent, J.-P. *Inorg. Chem*. **1990**, *29*, 2448. (c) Tweedle, M.; Wilson, L. J.; *J. Am. Chem. Soc*. **1976**, *98*, 4824.

(14) (a) Noveron, J. C.; Herradora, R.; Olmstead, M. M.; Mascharak, P. K. *Inorg. Chim. Acta* **1999**, *285*, 269. (b) Shoner, S. C.; Barnhart, D.; Kovacs, J. A. *Inorg. Chem*. **1995**, *34*, 4517. (c) Fallon, G. D.; Gatehouse, B. M. *J. Chem. Soc., Dalton Trans*. **1975**, 1344.

(15) Zang, Y.; Kim, J.; Dong, Y.; Wilkinson, E. C.; Appelman, E. H.; Que, L., Jr. *J. Am. Chem. Soc*. **1997**, *119*, 4197−4205.

(16) de Vries, M. E.; La Crois, R. M. L.; Roelfes, G.; Kooijman, H.; Spek, A. L.; Hage, R.; Feringa, B. L. *Chem. Commun*. **1997**, 1549.

(17) (a) Goedken, V. L.; Pluth, J. J.; Peng, S.-M.; Bursten, B. *J. Am. Chem. Soc*. **1976**, *98*, 8014. (b) Goedken, V. L.; Peng, S.-M.; Molin-Norris, J.; Park, Y. *J. Am. Chem. Soc*. **1976**, *98*, 8391.

(18) (a) Rauchfuss, T. B.; Contakes, S. M.; Hsu, S. C. N.; Reynolds, M. A.; Wilson, S. R. *J. Am. Chem. Soc*. **2001**, *123*, 6933. (b) Darensbourg, D. J.; Lee, W.-Z.; Yarbrough, J. C. *Inorg. Chem*. **2001**, *40*, 6533.

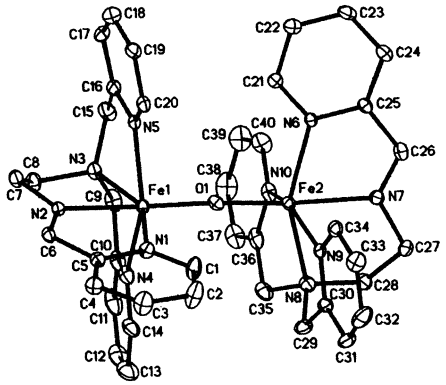

Figure 5. Thermal ellipsoid plot (35% probability level) of $[(SBPy_3)FeOFe(SBPy_3)]^{4+}$ (cation of **5**) with showing the atom numbering scheme. Hydrogen atoms are omitted for the sake of clarity.

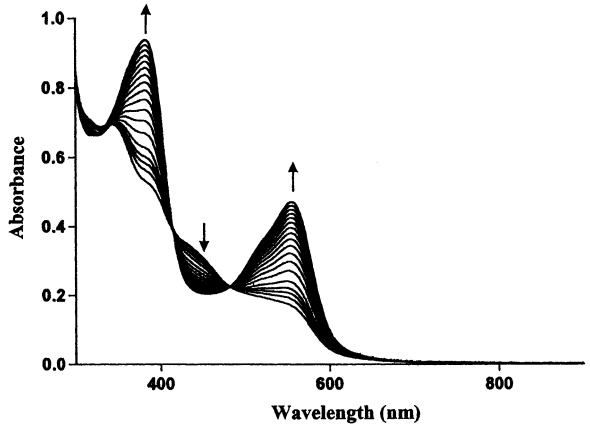

Figure 6. Electronic absorption spectra showing spontaneous reduction of $[(SBPy_3)Fe(DMF)](ClO_4)_3$ (**2**) to $[(SBPy_3)Fe(MeCN)](ClO_4)_2$ in MeCN. The spectra were taken at 10 min intervals.

presence of ligated CN^- around iron in **4** facilitates oxidation of the metal center to the +3 oxidation state. Thus, in MeCN, **4** exhibits a reversible cyclic voltammogram with an $E_{1/2}$ value of 0.69 V (vs SCE). The low-spin nature of the Fe(II) center in **4** is supported by its NMR spectrum (Figure S2, Supporting Information).

$[(SBPy_3)FeOFe(SBPy_3)](ClO_4)_4 \cdot 1.2(Me)_2CO \cdot 0.8H_2O$ (5·$1.2(Me)_2CO \cdot 0.8H_2O$). The structure of the cation of μ-oxo Fe(III) dimer **5** is shown in Figure 5, and selected bond distances and angles are listed in Table 3. Both Fe(III) centers exist in distorted octahedral geometry, and the Fe−O−Fe moiety is almost linear (Fe1−O1−Fe2 = 175.4(2)°). The conformation of the coordinated $SBPy_3$ ligand is very similar, and the imine nitrogens are trans to the bridging oxo group. Comparison of the metric parameters of **5** with those of $[(N4Py)FeOFe(N4Py)]^{4+}$ clearly indicates that the Fe(III) centers in **5** are high spin.[8e] For example, the average Fe(III)−N_{py} distance in **5** (2.137 Å) is very close to that observed in $[(N4Py)FeOFe(N4Py)]^{4+}$ (2.125 Å). Also, the Fe(III)−$N_{(tert\text{-amine})}$ distance in **5** (average: 2.219 Å) is close to that in $[(N4Py)FeOFe(N4Py)]^{4+}$ (2.244 Å). The trans influence of the bridging oxo group is reflected in the longer Fe(III)−N_{imine} distance (average distance is 2.142(5) Å).

Reactivity of $[(SBPy_3)Fe(DMF)](ClO_4)_3$ (2). As mentioned in a previous section, the $E_{1/2}$ value of **3** shows that $SBPy_3$, much like the ligands of Figure 1, stabilizes Fe(II) centers to a great extent. This stabilization imparts instability to corresponding Fe(III) complex **2**. The first sign of this instability becomes evident when one dissolves **3** in MeCN. The initial red color is changed to deep purple ($t_{1/2}$ = 100 min) showing *spontaneous reduction of the Fe(III) center* of **2**. This rapid conversion of $[(SBPy_3)Fe(DMF)]^{3+}$ to $[(SBPy_3)Fe(MeCN)]^{2+}$ upon mere dissolution in MeCN is quite striking. The spontaneous reduction of the Fe(III) center of **2** in MeCN has been monitored by spectrophotometry. As shown in Figure 6, the reduction of the Fe(III) center of **2** is indicated by rapid growth of two distinct peaks at 557 and 385 nm. Two isosbestic points at 480 and 416 nm suggest that the reduction is a clean one with **3** as the sole product. Also, the absence of significant absorption at 366 nm indicates that no oxo-bridged dimer **5** is present in the solution. In the present work, we have also synthesized **3** in high yield via spontaneous reduction of **2** in MeCN.

The spontaneous reduction of the Fe(III) center in **2** is driven by the unusual stability $SBPy_3$ provides to Fe(II) centers. Indeed, the ligands of Figure 1 all behave in a similar fashion. It has previously been reported that reaction of N4Py with both Fe(II) and Fe(III) salts affords Fe(II) complex $[(N4Py)Fe(MeCN)]^{2+}$ as the sole product.[8e] Also, the major part of the work done with ligands such as N4Py and PY5 has been performed in solvents such as MeOH. Use of MeCN caused problems in all such studies. It is now evident these studies were beset with problems due to reduction of the iron centers in MeCN.

The reported mononuclear iron complexes of ligands of Figure 1 are mostly Fe(II) species. One can only synthesize Fe(III) complexes with these ligands in the presence of an anionic sixth ligand. For example, both $[(PY5)Fe(OMe)](OTf)_2$ and $[(N4Py)Fe(OMe)](ClO_4)_2$ have been synthesized as stable species.[8c,e] We have been successful in isolating Fe(III) species $[(SBPy_3)Fe(DMF)](ClO_4)_3$ (**2**) in the present work solely because the Fe(III) complex crystallizes out of methanolic solution within minutes after mixing. Spontaneous reduction of **2** to **3** also occurs in DMF albeit slowly. Finally, **2** is also not very stable in MeOH. When kept in MeOH as a dilute solution (**2** has limited solubility in MeOH), **2** is slowly converted into **5**. Similar behavior has been reported for N4Py complexes.[8e]

Another reactivity of **2** deserves attention. We have previously shown that the azomethine moiety of the type CH═N−py (py = pyridine), when coordinated to a M(III) center, is rather reactive and is readily converted into a coordinated pyridine-2-carboxamido (C(═O)−N−py) unit upon reaction with H_2O_2 (Scheme 1).[19] Complex **2** contains a coordinated CH═N−py moiety and hence exhibits similar reactivity. Reaction of **2** with H_2O_2 in MeCN rapidly converts it into complex **1**. The mechanism of the imine-to-carboxamide conversion has been discussed before.[19] Finally, one major difference between **1** and **2** should be mentioned. Although these two Fe(III) complexes only differ by the presence of a carboxamido nitrogen (in **1**) in place of an imine nitrogen (in **2**), the Fe(III) center in **1** binds NO[20] while

(19) Tyler, L. A.; Olmstead, M. M.; Mascharak, P. K. *Inorg. Chem.* **2001**, *40*, 5408 and references therein.

Scheme 1

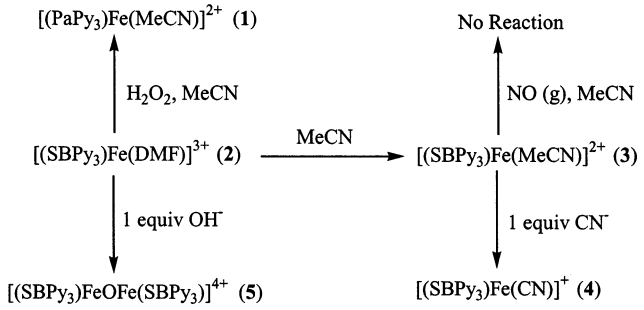

the Fe(III) center of **2** does not. Clearly, coordination of the negatively charged carboxamido nitrogen to the Fe(III) center in **1** and the consequent change in its redox potential are responsible for its affinity toward NO. The Fe(II) complex of $SBPy_3$, namely $[(SBPy_3)Fe(MeCN)](BF_4)_2$ (**3**), also does not bind NO under any condition. The various reactions of all the complexes of $SBPy_3$ are summarized in Scheme 1.

Summary and Conclusion

The following are the summary and conclusions of this work: (a) A new pentadentate Schiff base ligand, $SBPy_3$, with mixed nitrogen (pyridine N, *tert*-amine N, and imine N) donors has been synthesized. (b) Iron complexes $[(SBPy_3)Fe(DMF)](ClO_4)_3$ (**2**), $[(SBPy_3)Fe(MeCN)](BF_4)_2$ (**3**), $[(SBPy_3)Fe(CN)](BF_4)$ (**4**), and $[(SBPy_3)FeOFe(SBPy_3)](ClO_4)_4$ (**5**) have been isolated. The structures of **3**−**5** have been determined by crystallography while the structure of **2** has been confirmed on the basis of spectral data. (c) The $E_{1/2}$ value of **3** (1.01 V vs SCE) in acetonitrile indicates that $SBPy_3$ stabilizes the Fe(II) center to a great extent. Although the limited solubility of **2** in MeOH has allowed us to isolate this Fe(III) complex, it is quite unstable in solution and is spontaneously reduced to **3** in MeCN. (d) Reaction of H_2O_2 in MeCN readily oxidizes the azomethine moiety (CH═N−py) of **2** into a pyridine-2-carboxamido (C(═O)−N−py) unit and affords **1**, a complex previously reported by us.

Acknowledgment. Financial support from NSF (CHE 9818492) and NIH (GM 61636) is gratefully acknowledged. The Bruker SMART 1000 diffractometer was funded in part by an NSF Instrumentation Grant CHE-9808259.

Supporting Information Available: ^1H NMR spectra of **3** and **4** in CD_3CN (Figures S1, S2) and X-ray crystallographic data (in CIF format) and tables for the structure determination of complexes $[(SBPy_3)Fe(MeCN)](BF_4)_2 \cdot 1/3Et_2O \cdot 2/3MeOH$ (**3**·1/3Et_2O·2/3MeOH), $[(SBPy_3)Fe(CN)](BF_4) \cdot MeCN$ (**4**·MeCN), and $[(SBPy_3)FeOFe(SBPy_3)](ClO_4)_4 \cdot 1.2\ (Me)_2CO \cdot 0.8H_2O$ (**5**·1.2 $(Me)_2CO$·0.8H_2O). This material is available free of charge via the Internet at http://pubs.acs.org.

IC020373W

(20) Patra, A. K.; Afshar, R.; Olmstead, M. M.; Mascharak, P. K. *Angew. Chem., Int. Ed.* **2002**, *41*, 2512.